



GEOQuébec
2015

Challenges from North to South
Des défis du Nord au Sud

On the stability of exposed backfill in mine stopes

Falaknaz, N.¹, Aubertin, M.², Li, L.²

¹BGC Engineering Inc, Vancouver, BC, Canada

²Research Institute on Mines and the Environment,

RIME UQAT-Polytechnique, École Polytechnique de Montréal, QC, Canada

ABSTRACT

Backfilling of mine stopes provides a safer work place. When exposed, the open face of cemented backfill must remain stable during removal of one of the support walls. The minimum strength of the backfill is a critical issue to avoid safety problems and reduce operational costs. This paper presents 3D numerical simulations results that illustrate the response of exposed backfill during sequential excavation, considering the effect of stope geometry and material strength. Numerical modelling results are then compared with analytical solutions to obtain the required backfill strength.

RÉSUMÉ

Le remblayage des chantiers miniers pour le contrôle du terrain autour de grandes ouvertures fournit un lieu de travail plus sécuritaire. La résistance minimale du remblai est une question cruciale pour éviter les problèmes de sécurité et pour économiser sur les coûts opérationnels. Cet article présente les résultats de simulations numériques en 3D visant à évaluer la réponse du remblai exposé pendant l'excavation séquentielle, en tenant compte de l'effet de la géométrie du chantier et de la résistance des matériaux. Les résultats de la modélisation numérique sont ensuite comparés avec des solutions analytiques pour obtenir la résistance requise du remblai cimenté.

1 INTRODUCTION

Backfilling is used to reduce ore dilution and the impact of mine wastes disposal on the surface. In addition to the environmental and economic benefits, backfilling can improve the stability of the rock mass around underground mine stopes (Hassani and Archibald 1998).

Some mining operations apply extraction methods that involve primary and secondary stopes in which the primary stopes are excavated and then filled with a cemented backfill. In this case, one of the walls can be removed and the backfill forming a "pillar" in the primary stope must be able to stand on its own. The stability of the exposed backfill face during adjacent mining is thus a critical issue to control the associated costs for the mining operation.

Mitchell et al. (1982) have proposed a limit equilibrium solution to estimate the required strength of cemented backfill placed in primary stopes with an open face. This solution based on the sliding of the wedge toward the exposed face of a vertical opening relies on a number of assumptions that may not all be realistic (e.g. Li and Aubertin, 2012, 2014). The solution proposed by Mitchell et al. (1982) was modified by Zou and Nadarajah (2006) to include the effect of a surcharge load. Dirige et al. (2009) also proposed an analytical solution to estimate the required strength of exposed backfill in an inclined stope, based on the same type of assumptions.

Li and Aubertin (2012) developed modified formulations, based on the Mitchell et al. (1982) model, considering backfilled stopes with a high aspect ratio (i.e. height $H \gg$ width B , as in the original solution) and a low aspect ratio, incorporating a surcharge on top of the backfill. This MM (Modified Mitchell) solution is recalled below, together with the original solution.

Numerical simulations have also been used to assess the response of primary backfilled stopes, considering the effect of dynamic loading (Emad and Mitri, 2013; Emad et al. 2014). Li and Aubertin (2014) used 3D simulations results to develop an alternate solution, which will also be presented below.

These numerical investigations have not considered key influence factors such as backfill properties, stope geometry, and excavation sequence. Also, the required backfill strength given by the analytical solutions mentioned above have not yet been compared with results from such 3D simulations.

In this paper, results from numerical calculations are presented to illustrate the effect of important factors, including stope size and fill properties, on the behavior and stability of exposed cemented backfill during mining of a secondary stope. The required strength obtained from numerical results is also compared with values given by the Mitchell et al. (1982) and Li and Aubertin (2012, 2014) solutions.

2 CONCEPTUAL MODEL AND BASIC CHARACTERISTICS

FLAC 3D (Itasca, 2014) is commonly used to analyze the stress state in backfilled stopes. This three-dimensional finite difference program can be used for modelling complex problems, with different constitutive models, material properties, and boundary conditions. The numerical analyses were performed to evaluate the effect of mesh size and boundary locations on the stresses and displacements. A planar symmetry model was built with a coarser mesh for elastic rock mass and a finer mesh inside the backfilled stopes. The number of elements and the global size of the model may vary with the openings geometry. In all cases, the external boundaries are

located far enough to avoid influence on the results (see details in Falaknaz, 2014).

The slope sidewalls are considered rough and irregular so that shearing tends to occur in the backfill. Therefore, the models do not include interface elements between the backfill and rock mass (as discussed by Li et al. 2003, Li and Aubertin 2009). Figure 1 shows the characteristics of the base model. The rock mass is considered homogeneous, isotropic and linearly elastic, with the following properties: $E_r = 30$ GPa (Young's modulus), $\nu_r = 0.3$ (Poisson's ratio), $\gamma_r = 27$ kN/m³ (unit weight). The backfill behaves as an elasto-plastic material and obeys Mohr-Coulomb criterion. A zero tensile strength cut-off was used in the following simulations (with a non-zero cohesion). The input properties for the backfill are the effective internal friction angle ϕ' , cohesion c' and dilatancy angle ψ' (i.e. with a non-associated flow rule), together with the other backfill characteristics (E , γ , and ν); these are summarized in Table 1 (adapted from Belem et al. 2000).

Table 1. Backfill properties and stope characteristics for the numerical simulations ($E = 300$ MPa, $\nu = 0.3$ and related $\phi' = 35^\circ$, $\gamma = 18$ kN/m³)

Cases (with variants)	B (m) (width)	L (m) (length)	H (m) (height)	c' (kPa) (cohesion)
1 _{9,10} , 1 _{9,30} 1 _{30,60} , 1 _{30,85}	6	9, 30	45	10, 30, 60, 85
2 _{25,20} , 2 _{25,30}	25	9	45	20, 30
3 _{25,20} , 3 _{25,24}	6	9	25	20, 24

The reference stope width is 6 m, and it is filled to a height of 45 m, with 0.5 m of void space left at the top. The natural in-situ vertical stress σ_v in the rock mass is based on the overburden weight, for a depth z of 300 m at the base of the stope. The natural in-situ horizontal stress σ_h is twice the vertical stress σ_v , based on a fairly typical situation encountered in the Canadian Shield (Arjang, 2004).

Natural stress state with gravity is the initial equilibrium condition applied for the vertical stress in the model (before creation of the first opening). Displacements are prevented along both axes at the base of the model while only vertical displacements are allowed on the sides of the model. In these simulations, the primary stope is excavated in one step and the rock wall convergence takes place. The backfill is then placed in this stope in four layers and wall displacements are registered. Then, one of the walls is removed in a single or multiple steps to create the secondary stope. The displacements of the front wall, back wall and two side walls are monitored during simulations. The backfill is considered fully drained, or dry (no pore water pressure) upon wall removal. A simulation continues until the model reaches an equilibrium condition or collapse of the fill. The stresses and displacements are determined along four vertical lines (Figure 1) in the primary backfilled stope, i.e. line

AA' (vertical central line, VCL), BB' (side wall), CC' (back wall) and DD' (open face). The strength to stress ratio (equivalent to the factor of safety FS) is determined using the zone averaged effective shear stress and the yield strength given by the model (based on the Mohr-Coulomb criterion) as supplied by FLAC3D.

3 STRESS STATE IN PRIMARY STOPE

Simulations have been conducted to study the response of primary backfilled stope after front wall removal. The effect of different characteristics including the stope length L , width B and height H , was investigated by considering different cohesion values (which control backfill strength) to evaluate more specifically the stability of the backfill after removal of the front wall. The results can be presented in terms of normal stresses and total displacements within the primary stope, considering removal of the support wall.

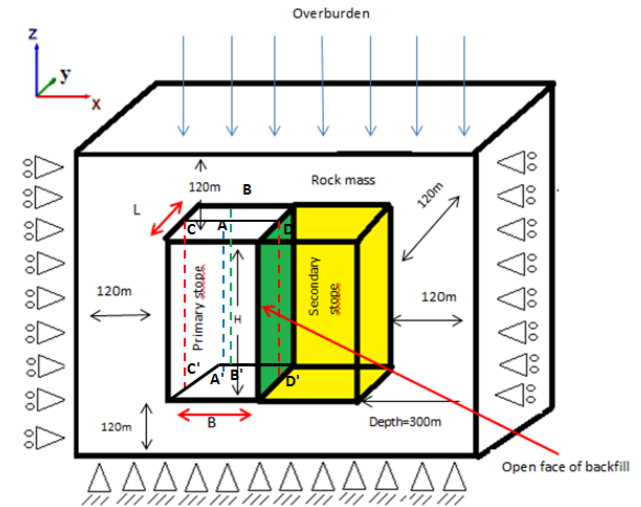


Figure 1. A schematic view of two adjacent stopes with the size and boundary conditions; the distance to the external boundaries is also given (not to scale);

3.1 Stopes with different lengths

The influence of stope length L (m) on the response of an exposed backfill is evaluated for stopes having a width of $B = 6$ m (Case 1, Table 1). The simulation results obtained for stopes with a length $L = 9$ m and $c' = 10$ kPa (Case 1_{9,10}, Table 1) or $c' = 30$ kPa (Case 1_{9,30}) and for $L = 30$ m and $c' = 60$ kPa (Case 1_{30,60}) or $c' = 85$ kPa (Case 1_{30,85}) are presented in the following.

Figure 2 shows the isocontours of the horizontal (S_{xx}) stresses (see orientations in Figure 1) obtained along vertical plane C'A'D'-DAC (center of the stope, Figure 1) within the primary stope before (BWR, left side) and after (AWR, right side) front wall removal. As expected, the results shown in Figure 2a (stable backfill) indicate that the reduction of the horizontal stresses due to arching, observed BWR when the 4 walls are in place, becomes less significant after removal of the front wall. The effect of the four layers used for filling the primary stope can also be seen in this figure. The situation illustrated in Figure

2b, where the weaker backfill becomes unstable AWR leads to significantly different results in this case.

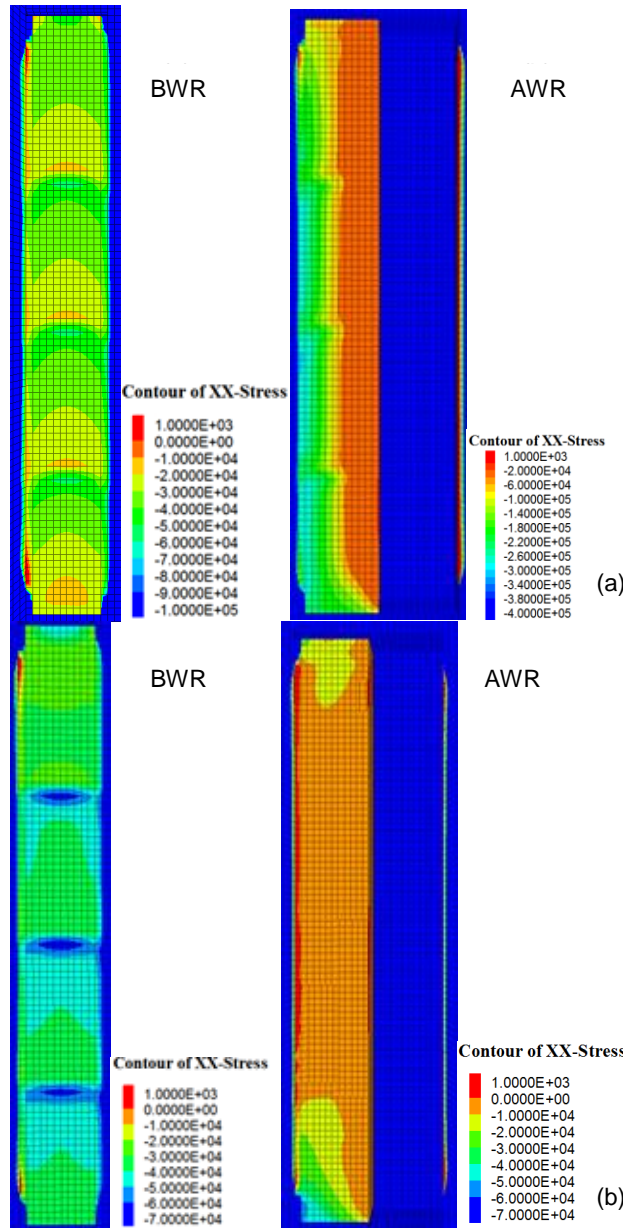


Figure 2. Horizontal (S_{xx}) stresses along the vertical plane C'A'D'-DAC (Figure 1) in the primary backfilled stope before (BWR) and after (AWR) front wall removal: (a) with $c' = 30$ kPa, (Case 1_{9,30}, stable backfill); (b) with $c' = 10$ kPa (Case 1_{9,10}, unstable backfill)

Figure 3 shows the horizontal stresses (S_{xx}) along the VCL (line AA' in Figure 1) and the three walls (lines BB', CC', DD') within the primary stope when $c' = 30$ kPa (Case 1_{9,30}) before (BWR) and after (AWR) removal of the front wall. In this case, the backfill remains stable upon removal of the front wall; stability is also confirmed when looking at the displacements, as will be shown below (see Figure 4 presented in the following).

It is seen that the horizontal stress S_{xx} , at mid-height, along the back wall (line CC') increases by up to 2 times (i.e. from $S_{xx} = 23$ kPa BWR to $S_{xx} = 54$ kPa AWR); along the side walls (line BB'), it increases by up to 5 times (from $S_{xx} = 15$ kPa BWR to $S_{xx} = 77$ kPa AWR). However, this horizontal stress (at mid-height) tends to decrease along the stope VCL, by up to 45% (from $S_{xx} = 18$ kPa BWR to $S_{xx} = 10$ kPa AWR). These results show that when the exposed backfilled face is stable, the horizontal stresses S_{xx} (and also S_{yy} , not shown here; see Falaknaz 2014) along the walls BWR tend to increase as a result of removing the front wall. Part of the stresses carried along the wall being removed is thus transferred to the remaining walls after creation of the adjacent stope.

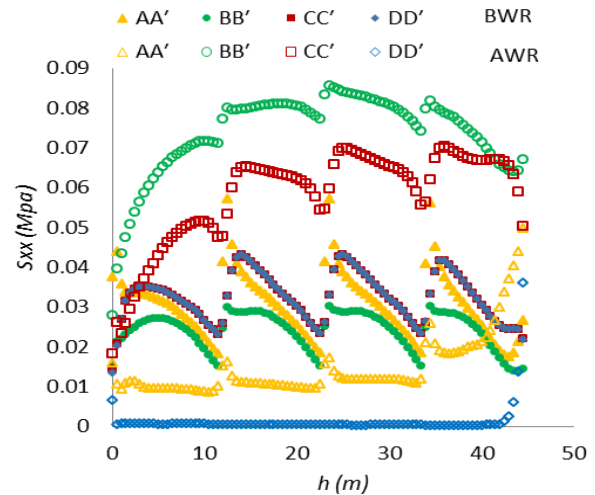


Figure 3. Horizontal stresses (S_{xx}) along the VCL (line AA'), back wall (line CC'), sidewalls (line BB') and open face (line DD') of the primary backfilled stope before (BWR) and after (AWR) front wall removal (Case 1_{9,30}, stable backfill).

Other simulations (results not shown here) analyzed the stresses for the same stope, but for a backfill with $c' = 10$ kPa (Case 1_{9,10}; see Falaknaz, 2014). In this case, the backfill was unstable upon removal of the front wall. The results indicate that the horizontal S_{xx} (normal) stresses decrease significantly (to less than 1 kPa) after the front wall removal, along the back wall (line CC') and along the side walls (line BB'). The horizontal stresses S_{yy} also decrease along the walls.

Figure 4 shows the total displacements of the backfill and the movement (arrows) of the front wall (AWR) for $L = 9$ m, with $c' = 30$ kPa (Figure 4a) and $c' = 10$ kPa (Figure 4b). The effect of the four layers used for filling the primary stope can be also seen in Figure 4a (as was also the case for the stresses shown in Figure 3). These results confirm that the backfill becomes unstable AWR when the cohesion is 10 kPa (Case 1_{9,10}), with the maximum (total) displacement of the open face δ_{max} reaching about 5 m (Figure 4b). The backfill remains stable when the cohesion is 30 kPa (Case 1_{9,30}) with $\delta_{max} = 3.5$ mm (Figure 4a). The angle of the sliding plane α at the base of the unstable backfilled stope, obtained from the simulation results, is about 56° (Figure 4b).

Figure 5 shows the horizontal stresses S_{xx} along the VCL and the three walls within a primary stoppe having a length, $L = 30$ m for $c' = 85$ kPa (Case 1_{30,85}) before (BWR) and after (AWR) removal of the front wall. The backfill remains stable in this case, contrarily to a backfill with $c' = 60$ kPa (Case 1_{30,60}, illustrated in Figure 6; detailed results in Falaknaz, 2014). It can be seen in Figure 5 that the final horizontal (normal) stresses along the VCL and back wall (AWR) are much smaller than those obtained before wall removal (BWR).

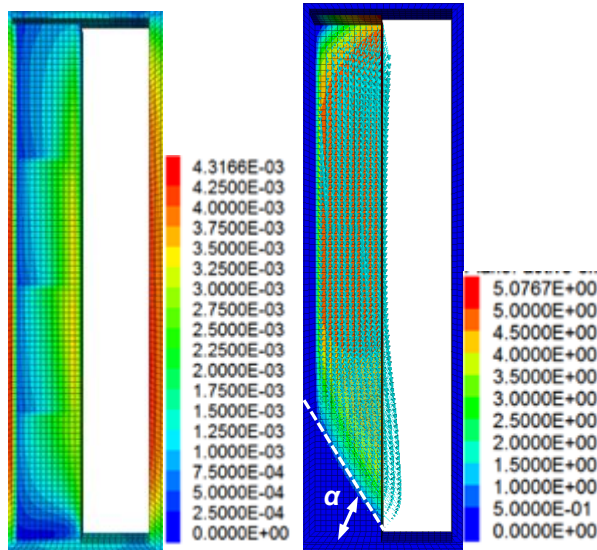


Figure 4. Total displacement isocontours in the primary backfilled stoppe ($L = 9$ m) after (AWR) front wall removal: (a) Case 1_{9,30}, stable backfill (b) Case 1_{9,10}, unstable backfill

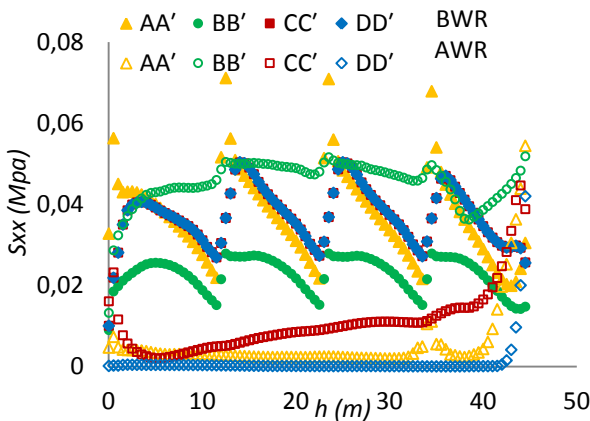


Figure 5. Horizontal stresses (S_{xx}) in the primary backfilled stoppe along the VCL (line AA'), back wall (line CC'), sidewalls (line BB') and open face (line DD') before (BWR) and after (AWR) front wall removal (Case 1_{30,85}, stable backfill)

Figure 6 presents the total displacements in the backfill for $L = 30$ m for two cohesion values, i.e. $c' = 85$ kPa (Case 1_{30,85}, Figure 6a) and 60 kPa (Case 1_{30,60},

Figure 6b). These results confirm that the backfill becomes unstable upon wall removal when the cohesion is 60 kPa; in this case, the maximum total displacement δ_{max} reaches 0.88 m (Figure 6b) near the top of the stoppe; the angle of the sliding plane at the base is about 53° . The backfill remains stable when the cohesion is 85 kPa (Case 1_{30,85}), with $\delta_{max} = 0.077$ m (Figure 6a).

3.2 Stopes with different widths

The effect of stoppe width B (m) on the response of an exposed backfill is evaluated for stoppes having a length $L = 9$ m and height $H = 45$ m (Case 2, Table 1), considering a stoppe width $B = 25$ m, for $c' = 30$ kPa (Case 2_{25,30}, Table1) or $c' = 20$ kPa (Case 2_{25,20}, Table1).

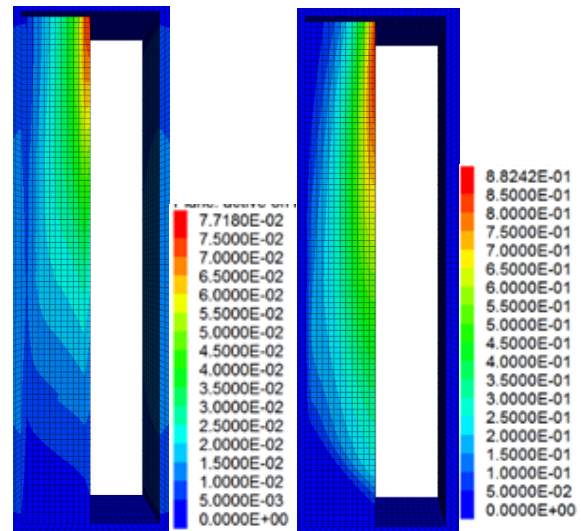


Figure 6. Total displacement contours along plane C'A'D'-DAC (Figure 1) in the primary backfilled stoppe after (AWR) front wall removal: (a) Case 1_{30,85}, stable backfill (b) Case 1_{30,60}, unstable backfill

Figure 7 shows the total displacements of the backfill after removal of the front wall (AWR) for $B = 25$ m, with $c' = 30$ kPa (Figure 7a, Case 2_{25,30}) and $c' = 20$ kPa (Figure 7b, Case 2_{25,20}). These results confirm that the backfill is stable when the cohesion equals 30 kPa, with the maximum (total) displacement of the open face $\delta_{max} = 9$ mm, while it is unstable when the cohesion is 20 kPa with $\delta_{max} = 1.4$ m (Figure 7b). The angle of the sliding plane α at the base of the unstable backfill is about 64° (Figure 7b), which is close to the value postulated by Mitchell et al. (1982) (i.e. $\alpha = 45^\circ + \phi'/2 = 62.5^\circ$ for $\phi' = 35^\circ$). These simulations results confirm that the stability of an exposed backfill face can be sensitive to the stoppe width, when the cohesion is low.

3.3 Stopes with different heights

The effect of stoppe height, H (m), on the response of exposed backfilled was also investigated, considering stoppes having a length $L = 9$ m, a width $B = 6$ m and a height $H = 25$ m (Case 3, Table 1). The simulations

results shown here were obtained for $c' = 24$ kPa (Case 3_{25,24}) and $c' = 20$ kPa (Case 3_{25,20}).

Figure 8 shows the total displacements of the backfill AWR, for $H = 25$ m, with $c' = 24$ kPa (Case 3_{25,24}, Figure 8a) and $c' = 20$ kPa (Case 3_{25,20}, Figure 8b). These results indicate that the backfill remains stable when $c' = 24$ kPa, with maximum (total) displacement of the open face $\delta_{max} = 4$ mm, near the top, while it becomes unstable when cohesion $c' = 20$ kPa, with $\delta_{max} = 0.44$ m. The effect of the four layers used for filling the primary slope can also be seen in this figure. These simulations results tends to confirm that the stability of the exposed backfill decreases with an increase of the slope height, for a given cohesion value.

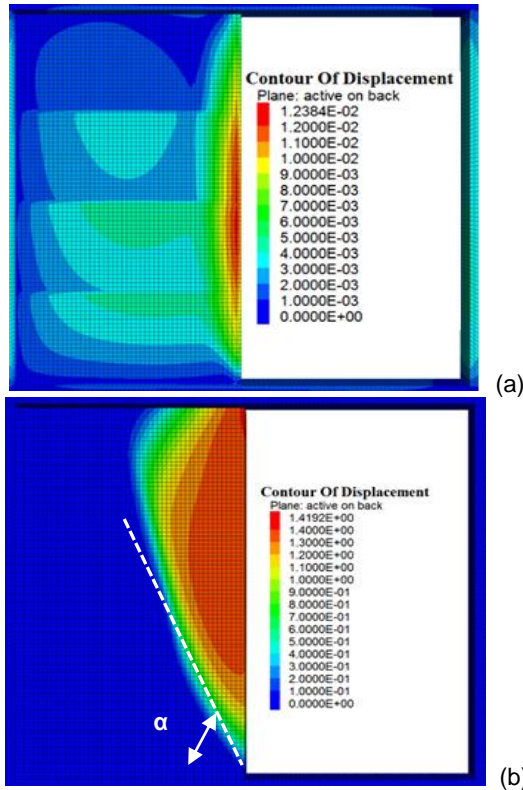


Figure 7. Total displacement contours along plane C'A'D'-DAC (Figure 1) in the primary backfilled stope after (AWR) front wall removal: (a) Case 2_{25,30}, stable backfill (b) Case 2_{25,20}, unstable backfill

4 COMPARISON WITH ANALYTICAL SOLUTIONS

Various analytical solutions have been proposed to estimate the strength of exposed backfill. Mitchell et al. (1982) developed the most commonly used analytical solution, which gives the factor of safety FS of an exposed backfill in a vertical stope (based on the model shown in Figure 9).

In addition to FS, this solution can also be used to evaluate the required cohesion c (kPa) for the backfill to be placed in a stope with an open face as follows:

$$c = \frac{\gamma H}{2 \left(\frac{H}{L} + \tan \alpha \right)} \quad \text{for } FS=1 \quad \phi = 0 \quad [1]$$

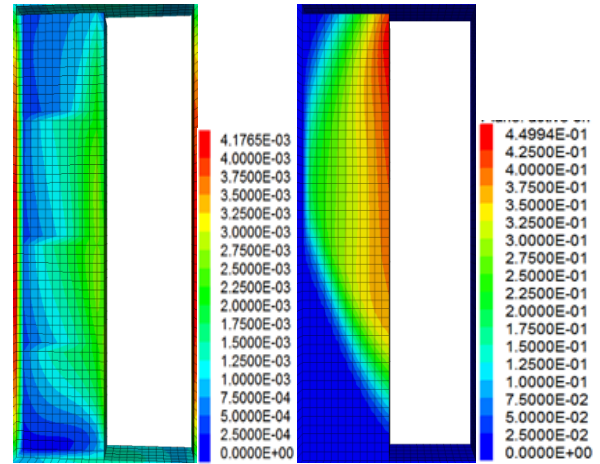


Figure 8. Total displacement contours along plane C'A'D'-DAC (Figure 1) in the primary backfilled stope after (AWR) front wall removal: (a) Case 3_{30,26}, stable backfill (b) Case 3_{30,20}, unstable backfill

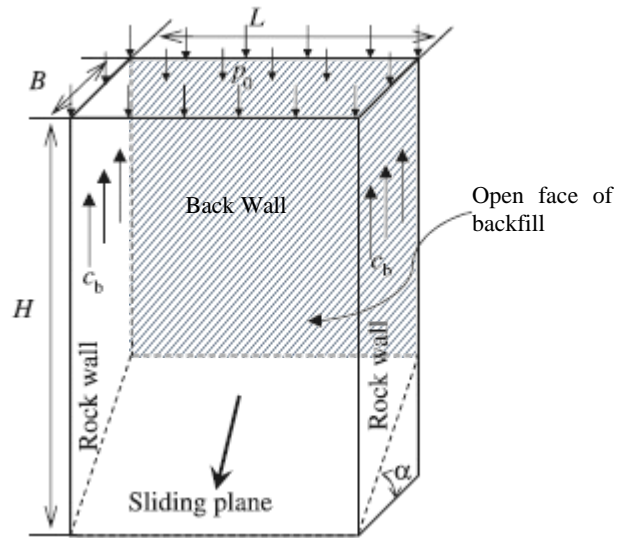


Figure 9. Wedge block model for the backfilled stope with an open face (after Mitchell et al. 1982).

In this equation, α is the angle of failure plane from the horizontal axis ($\alpha = 45^\circ + \phi / 2$ is assumed); ϕ is internal friction angle ($^\circ$) of the backfill material; γ is the fill unit weight (kN/m^3); L is the exposed block length (m); H is the block height (m). This solution applies to backfilled stopes with a high aspect ratio (i.e. $H \gg B$) and when the cohesion along the interfaces between the backfill and two side walls is equal to the cohesion of the backfill.

Li and Aubertin (2012) modified the Mitchell et al. (1982) solution, using many of the same assumptions. However, they postulated that the cohesion along the two lateral interfaces between the backfill and the sidewalls could be smaller than the backfill cohesion. This led to the

following MM solution for stopes with a high aspect ratio (HAR):

$$c = \frac{(p_o + \gamma(H - (B \times \tan \alpha)/2))/2}{\left[\left(FS - \frac{\tan \phi}{\tan \alpha} \right) \sin 2\alpha \right]^{-1} + r_b \left(H - \frac{B \times \tan \alpha}{2} \right)/L} \quad [2]$$

Where r_b ($= c_b/c$; from 0 to 1) is the adherence ratio of the fill-rock interface over the backfill cohesion.

More recently, Li and Aubertin (2014) presented numerical simulations results obtained with FLAC3D that illustrate the response of exposed backfill in terms of displacements. The results were used to develop the following solution:

$$c = \frac{D'(p_o + \gamma(H - H') - G') + \frac{(A' \gamma H')}{2} [1 + L/B] \sin \alpha - \gamma \left(\frac{C'}{M} + \frac{H'}{2} \right)}{\left(1 + \frac{L}{B} \right) B' + D'(H - H') \left(\frac{2r_{bs}}{L} + \frac{r_{bb}}{B} \right)} \quad [3]$$

With

$$p_1 = p_o - G' + (H - H') \left\{ \gamma - c \left(\frac{2r_{bs}}{L} + \frac{r_{bb}}{B} \right) \right\} \quad [4]$$

$$G' = \frac{1}{1 + \frac{L}{B}} \left\{ \gamma(H - H') + \left(p_o - \frac{\gamma}{M} \right) [1 - \exp(-(H - H')M)] \right\}$$

[5]

$$A' = FS - \frac{\tan \phi}{\tan \alpha} \quad B' = \frac{1}{\cos \alpha} + r_{bs} \frac{H'}{L} \quad C' = \frac{1 - \exp(-MH')}{MH'} - 1$$

$$D' = A' \left(1 + \frac{L}{B} \right) \sin \alpha + C' \quad H' = B \tan \alpha \quad [6]$$

$$M = 2K (B^{-1} + L^{-1}) \tan \delta \quad [7]$$

In these equations, the interface cohesion, c_{bb} , along the back wall is proportional to the backfill cohesion, ($c_{bb} = r_{bb} \cdot c$; parameter r_{bb} controls the interface cohesion along the back wall in the model ($0 \leq r_{bb} \leq 1$). A similar parameter r_{bs} is used for the interface cohesion between the backfill and the side walls (i.e. $c_{bs} = r_{bs} \cdot c$, with $0 \leq r_{bs} \leq 1$). In the above equations, K is an earth reaction coefficient, which is considered equal to Rankine's active earth pressure (K_a) and δ is the friction angle ($^\circ$) along the fill-wall interfaces. This solution considers the possibility of having frictionless ($\delta = 0$) or fully frictional interfaces ($\delta = \phi$) along the walls (or intermediate situations).

A series of numerical simulations have been conducted to evaluate the stability of exposed backfill for different conditions and to assess the validity of the three analytical solutions presented above. In these simulations, the tension cut-off for the backfill strength (Mohr-Coulomb criterion) is considered nil on the tensile stresses side (which is a conservative assumption).

Figure 10 shows the variation of the required backfill cohesion c' (for $FS = 1$) obtained from the Mitchell et al. (1982) solution, the MM solution from Li and Aubertin (2012), and the Li and Aubertin (2014) solution when $r_{bb} = r_{bs} = 1$, (rough walls). The simulations were repeated for different geometries by varying the value of c' to determine the backfill cohesion required to maintain a stable condition; this critical value is obtained by the strength reduction method, from one simulation to the other, until failure appears. The displacements and stresses are monitored during each simulation to assess

the stability of the model. The results shown in Figure 10 illustrate the effect of varying the length L . Other calculations have also been performed to assess the effect of width B and height H (details in Falaknaz, 2014). The minimum required cohesion obtained from the three analytical solutions is also shown in Figure 10.

The simulations results indicate that the required backfill strength, c' (for a fixed internal friction angle $\phi' = 35^\circ$), increases with an increase of the stope length L (and with height H , as shown by other results); additional simulations also show that the required cohesion c' remains almost constant when stope width B varies (Falaknaz, 2014). For the base cases (performed with a zero tension cut-off), the cohesion value given by the solution of Li and Aubertin (2014) is the closest to the numerical results (i.e. with the starting value for L , B and H). However, the tendencies observed in Figure 10 and in other simulations results do not always agree with those of the analytical solutions.

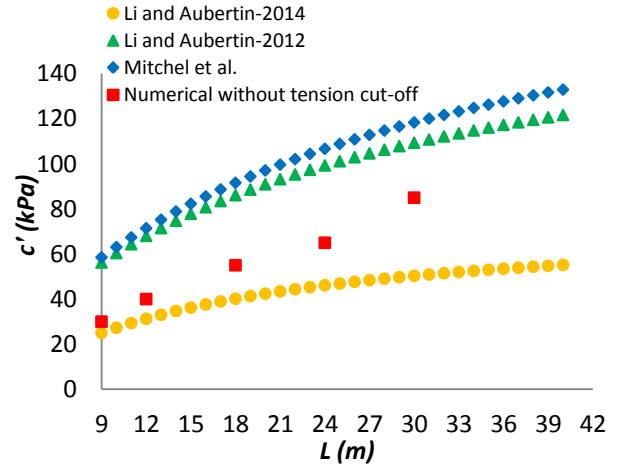


Figure 10. Required backfill cohesion c' (for $FS = 1$) as a function of the stope length, L , ($H = 45\text{m}$, $B = 6\text{ m}$). Results obtained from three analytical solutions and numerical simulations.

More specifically, the Li and Aubertin (2014) solution seems to better capture the effect of H (not shown here), while the effect of L follows an intermediate trend between this solution and the MM solution (Figure 10). The MM and Mitchell et al. (1982) solutions tend to overestimate the required strength, while the cohesion given by that of Li and Aubertin (2014) is underestimated when L is increased. Other simulations results indicate that the required strength does not change much with the stope width B , hence following the trend given by the Mitchell et al. (1982) solution, which nonetheless tends to overestimate the required cohesion.

It thus appears, based on these numerical simulations, that the three solutions considered here don't fully capture the variation of the required cohesion as a function of the stope geometry. More work is thus required to better define the critical value of cohesion for various geometrical characteristics of mine stopes with exposed backfill.

5 CONCLUSION

This article presents some of the main results of a numerical and analytical investigation of the behavior of exposed backfill in mine stopes (with an open face). The results from this investigation show that higher backfill strength is required for stopes with a higher length or height, while the stability of the exposed backfill face appears to be little affected by the stope width. The results also indicate that non-negligible contact stresses exist along the fill-wall interfaces, on the three remaining walls, after front wall removal. This observation is not in line with the assumptions behind the development of the analytical solutions proposed by Mitchell et al. (1982) and Li et al. (2012, 2014). The backfill behavior thus needs to be reconsidered to obtain a more representative solution for the required strength of cemented backfill.

6 ACKNOWLEDGEMENTS

The authors acknowledge the financial support from NSERC, from the partners of the Industrial NSERC Polytechnique-UQAT Chair on Environment and Mine Wastes Management (2006-2012), and from the Research Institute on Mines and the Environment (RIME UQAT-Polytechnique; www.rime-irme.ca).

7 REFERENCES

- Arjang, B. 2004. Database on Canadian in situ ground stresses. CANMET Division Report MMSL, 01-029 (TR).
- Belem, T., Benzaazoua, M., and Bussi re, B. 2000. Mechanical behaviour of cemented paste backfill. In Proceedings of 53th Canadian Geotechnical Conference, Montreal, Canada, Vol. 1, pp. 373-380.
- Dirige APE, McNearny RL, Thompson DS. 2009. The effect of stope inclination and wall rock roughness on back-fill free face stability. In: Rock Engineering in Difficult Conditions: Proceedings of the 3rd Canada-US Rock Mechanics Symposium, Toronto, 2009: 9-15.
- Emad, M.Z., Mitri, H.S. 2013. Modelling dynamic loading on backfilled stopes in sublevel stoping systems. Rock characterisation, modelling and engineering designs methods, Feng Hudson and Tan (Eds), Taylor and Francis Group, London, ISBN 978-1-138-00057-5.
- Emad, M.Z., Mitri, H.S., and Kelly, C. 2014. Effect of blast-induced vibration on fill failure in vertical block mining with delayed backfill. *Can. Geotech. J.* 51(9): 975-983.
- Falaknaz, N. 2014. Analysis of the geomechanical behavior of two adjacent backfilled stopes based on two and three dimensional numerical simulations, PhD thesis, Polytechnique Montreal
- Hassani, F., and Archibald, J. 1998. Mine backfill. CD-Rom, Canadian Institute of Mine, Metallurgy and Petroleum. Montreal, CIM.
- Itasca. 2014. FLAC3D version 5.0. Users Manuals. ITASCA Consulting Group, Thresher square East, 708 South Third Street, Suite 310, Minneapolis, Minnesota, USA.
- Li, L., Aubertin, M., and Belem, T. 2005. Formulation of a three dimensional analytical solution to evaluate stress in backfilled vertical narrow openings. *Can. Geotech. J.*, 42(6), 1705-1717.
- Li, L., and Aubertin, M. 2009. Numerical investigation of the stress state in inclined backfilled stopes. *International Journal of Geomechanics*, 9(2): 52-62.
- Li L, Aubertin M. 2012. A modified solution to assess the required strength of exposed backfill in mine stopes. *Can Geotech J*, 49(8): 994-1002.
- Li L, Aubertin M. 2014. An improved method to assess the required strength of cemented backfill in underground stopes with an open face. *International Journal of Mining Science and Technology*, 24 : 549–558.
- Mitchell, R.J., Olsen, R.S., and Smith, J.D. 1982. Model studies on cemented tailings used in mine backfill. *Canadian Geotechnical Journal*, 19(1): 14–28. doi:10.1139/t82-002.
- Zou, D.H., and Nadarajah, N. 2006. Optimizing backfill design for ground support and cost saving. In Proceedings of the 41st U.S. Rock Mechanics Symposium – ARMA’s Golden Rocks 2006 – 50 Years of Rock Mechanics, Golden, Colo. Omnipress.